

# Gravitating monopoles and black holes at intermediate Higgs masses

Yves Brihaye

Faculté des Sciences, Université de Mons-Hainaut, B-7000 Mons, Belgium

and

Betti Hartmann, Jutta Kunz

Fachbereich Physik, Universität Oldenburg, D-26111 Oldenburg, Germany  
(October 8, 2018)

Self-gravitating SU(2) Higgs magnetic monopoles exist up to a critical value of the ratio of the vector meson mass to the Planck mass, which depends on the Higgs boson mass. At the critical value a critical solution with a degenerate horizon is reached. As pointed out by Lue and Weinberg, there are two types of critical solutions, with a transition at an intermediate Higgs boson mass. Here we investigate this transition for black holes, and reconsider it for the case of gravitating monopoles.

## I. INTRODUCTION

In the SU(2)-Einstein-Yang-Mills-Higgs model, gravitating magnetic monopoles and non-abelian black holes exist in a certain region of the parameter space [1–3]. For a fixed value of the Higgs boson mass, gravitating monopoles exist up to a critical value  $\alpha_{\text{cr}}$  (of the parameter  $\alpha$ , which is proportional to the ratio of the vector meson mass to the Planck mass), and non-abelian black holes exist up to a critical value  $\alpha_{\text{cr}}(x_h)$  (for small enough values of the horizon radius  $x_h$  [3]). At the critical value  $\alpha_{\text{cr}}$  a critical solution with a degenerate horizon is reached. In particular, for small values of the Higgs boson mass, the critical solution where a horizon first appears corresponds to an extremal Reissner-Nordstrøm (RN) solution outside the horizon while it is non-singular inside.

Recently Lue and Weinberg [4] reconsidered self-gravitating magnetic monopoles. In particular, they observed, that for larger values of the Higgs boson mass, the critical solution is an extremal black hole with non-abelian hair and a mass less than the extremal RN value. Exploring the transition between the two regimes, occurring at some intermediate value of the Higgs boson mass, Lue and Weinberg were left with a discrepancy between their analytical and numerical results [4].

Here we extend the investigation of Lue and Weinberg to non-abelian black holes, showing the transition to persist in the presence of fixed finite event horizon radii  $x_h$ . Furthermore, we reconsider the case of gravitating monopoles and argue, that the discrepancy between Lue and Weinberg’s analytical and numerical results [4] can be traced back to their limited numerical analysis.

## II. EQUATIONS OF MOTION

We consider the SU(2) Einstein-Yang-Mills-Higgs action, with a Higgs triplet [1–6]

$$S = \int \frac{1}{16\pi G} R \sqrt{-g} d^4x - \int \left[ \frac{1}{4} F_{\mu\nu}^a F^{a\mu\nu} + \frac{1}{2} D_\mu \phi^a D^\mu \phi^a + \frac{1}{4} \lambda (\phi^a \phi^a - v^2)^2 \right] \sqrt{-g} d^4x \quad (1)$$

where

$$F_{\mu\nu}^a = \partial_\mu A_\nu^a - \partial_\nu A_\mu^a + e \epsilon^{abc} A_\mu^b A_\nu^c, \quad (2)$$

$$D_\mu \phi^a = \partial_\mu \phi^a + e \epsilon^{abc} A_\mu^b \phi^c, \quad (3)$$

$e$  is the gauge coupling constant,  $\lambda$  is the Higgs coupling constant and  $v$  is the Higgs field vacuum expectation value. Variation of the action eq. (1) with respect to the metric  $g_{\mu\nu}$ , the gauge field  $A_\mu^a$  and the Higgs field  $\phi^a$  leads to the Einstein equations and the matter field equations.

To construct static spherically symmetric globally regular and black hole solutions we employ Schwarzschild-like coordinates and adopt the spherically symmetric metric [5,6]

$$ds^2 = g_{\mu\nu} dx^\mu dx^\nu = -A^2 N dt^2 + N^{-1} dr^2 + r^2(d\theta^2 + \sin^2 \theta d\phi^2) , \quad (4)$$

with the metric functions  $A(r)$  and  $N(r)$ ,

$$N(r) = 1 - \frac{2m(r)}{r} , \quad (5)$$

where  $m(r)$  is the mass function.

For the gauge and Higgs fields we employ the standard spherically symmetric ansatz with vanishing time component of the gauge field [1-4]

$$\vec{A}_t = 0 , \quad \vec{A}_r = 0 , \quad \vec{A}_\theta = -\vec{e}_\phi \frac{1 - K(r)}{e} , \quad \vec{A}_\phi = \vec{e}_\theta \frac{1 - K(r)}{e} \sin \theta , \quad (6)$$

and

$$\vec{\phi} = \vec{e}_r H(r) v , \quad (7)$$

with unit vectors  $\vec{e}_r$ ,  $\vec{e}_\theta$  and  $\vec{e}_\phi$ .

We now introduce the dimensionless coordinate  $x$  and the dimensionless mass function  $\mu$ ,

$$x = evr , \quad \mu = evm , \quad (8)$$

as well as the coupling constants  $\alpha$  and  $\beta$ ,

$$\alpha^2 = 4\pi G v^2 , \quad \beta^2 = \frac{\lambda}{g^2} . \quad (9)$$

The  $tt$  and  $rr$  components of the Einstein equations then yield the equations for the metric functions,

$$\mu' = \alpha^2 \left( NK'^2 + \frac{1}{2} Nx^2 H'^2 + \frac{(K^2 - 1)^2}{2x^2} + H^2 K^2 + \frac{\beta^2}{4} x^2 (H^2 - 1)^2 \right) , \quad (10)$$

and

$$A' = \alpha^2 x \left( \frac{2K'^2}{x^2} + H'^2 \right) A , \quad (11)$$

where the prime indicates the derivative with respect to  $x$ . For the matter functions we obtain the equations

$$(ANK')' = AK \left( \frac{K^2 - 1}{x^2} + H^2 \right) , \quad (12)$$

and

$$(x^2 ANH')' = AH (2K^2 + \beta^2 x^2 (H^2 - 1)) . \quad (13)$$

The equations of motion depend only on the two physical parameters  $\alpha$  and  $\beta$ , eq. (9). They are related to the parameters  $a$  and  $b$  employed by Lue and Weinberg [4] via

$$a = 2\alpha^2 = 8\pi G v^2 , \quad b = \frac{1}{2}\beta^2 = \left( \frac{m_H}{2m_W} \right)^2 . \quad (14)$$

We note that the embedded RN solution with mass  $\mu_\infty$  and unit magnetic charge

$$\mu(x) = \mu_\infty - \frac{\alpha^2}{2x} , \quad A(x) = 1 , \quad K(x) = 0 , \quad H(x) = 1 . \quad (15)$$

is a special solution of these equations. The extremal RN solution, in particular, has horizon  $x_h$ ,

$$x_h = x_0 = \mu_\infty = \alpha . \quad (16)$$

### III. GRAVITATING MONOPOLES

Let us first consider the globally regular particle-like solutions of the SU(2) EYMH system, the gravitating monopoles. Requiring asymptotically flat solutions implies that the metric functions  $A$  and  $\mu$  both approach a constant at infinity. We here adopt

$$A(\infty) = 1 , \quad (17)$$

and  $\mu(\infty) = \mu_\infty$  represents the dimensionless mass of the solutions. The matter functions also approach constants asymptotically,

$$K(\infty) = 0 , \quad H(\infty) = 1 . \quad (18)$$

Regularity of the solutions at the origin requires

$$\mu(0) = 0 , \quad K(0) = 1 , \quad H(0) = 0 . \quad (19)$$

Let us now recall how the gravitating magnetic monopole solutions approach critical solutions, when the vector boson mass, i.e.  $a$ , is varied, while the ratio of the Higgs boson mass to the vector boson mass, i.e.  $b$ , is kept fixed. We focus on intermediate values of  $b$ .

Lue and Weinberg [4] realized that there are two regimes of  $b$ , each with its own type of critical solution. In the first regime  $b$  is small. Here the metric function  $N(x)$  of the monopole solutions always possesses a single minimum. With increasing  $a$  the minimum of the function  $N(x)$  decreases. For  $a \rightarrow a_{\text{cr}}$ , the critical solution is approached, where the minimum of the function  $N(x)$  reaches zero at  $x = x_0$ , eq. (16). For  $x \geq x_0$  the critical solution corresponds to an extremal RN black hole solution with horizon radius  $x_h = x_0$  and unit magnetic charge, eq. (15). Consequently, the mass of the limiting solution coincides with the mass of this extremal RN black hole, eq. (16). However, in the interior region,  $x < x_0$ , the critical solution is not singular, in particular  $N(0) = 1$ . We refer to this approach to the critical solution as RN-type behaviour. RN-type behaviour was seen for gravitating monopoles and black holes [1–3] as well as for gravitating dyons and dyonic black holes [5,6].

In the newly found [4] second regime  $b$  is large, and the metric function  $N(x)$  of the monopole solutions develops a second minimum as the critical solution is approached. This second minimum arises interior to the location of the first minimum, the solution therefore now possesses an inner and an outer minimum. Once present, the inner minimum decreases faster with increasing  $a$  than the outer minimum. Consequently, the inner minimum reaches zero, when the outer minimum still has a finite value, which is indeed not too different from the value it had, when the inner minimum first appeared. Thus for  $a \rightarrow a_{\text{cr}}$ , the inner minimum of  $N(x)$  reaches zero at  $x = x_* < x_0$ . This second approach to the critical solution is demonstrated in Fig. 1, where we show the function  $N(x)$  for  $b = 36.125$  and several values of  $a$  close to  $a_{\text{cr}}$ . Here the critical solution possesses an extremal horizon at  $x_* < x_0$ , corresponding to an extremal black hole with non-abelian hair and a mass less than the extremal RN value. Consequently, we refer to this approach to the critical solution as NA-type (non-abelian-type) behaviour.

In their paper [4] Lue and Weinberg investigated analytically the transition from RN-type behaviour to NA-type behaviour. One of their central analytical results is, that RN-type behaviour is possible only for  $a > 1.5$ , making  $a_{\text{tr}} = 1.5$  the critical value, where the transition from RN-type to NA-type behaviour should occur. This lower bound is found by an accurate analytical expansion of the solution about the point  $x = x_0$ , where  $N(x)$  has a double zero. The hypotheses used are mild and, very likely, fulfilled by the solutions.

When investigating the transition from RN-type to NA-type behaviour numerically, Lue and Weinberg [4] observe, that with increasing  $b$  the critical value  $a_{\text{cr}}$  decreases. For small  $b$  the critical value  $a_{\text{cr}}$  is larger than the analytical transition value  $a_{\text{tr}}$ , and the behaviour is of RN-type as expected. As  $b$  is increased, and  $a_{\text{cr}}$  decreases towards  $a_{\text{tr}} = 1.5$  the behaviour remains of RN-type. ( $a_{\text{tr}} = 1.5$  would correspond to  $b \approx 25.6$  [4].) But surprisingly, as  $a_{\text{tr}} = 1.5$  is passed, Lue and Weinberg do not immediately observe the transition to NA-type behaviour. Instead they continue to see numerically RN-type behaviour until a value  $a_{\text{cr}} = 1.42$ , corresponding to  $b \approx 40$ , which is clearly below their analytical prediction for the transition.

Convinced by the analytical argument given by Lue and Weinberg [4] for the transition value, we argue in the following that the numerically observed discrepancy arises only because of their interpretation of their inaccuracy limited numerical analysis.

Performing an independent numerical analysis (see Appendix for details), we observe that NA-type behaviour occurs indeed for lower values of  $b$  than  $b = 40$  and thus larger values of  $a$  than  $a = 1.42$ . Numerically we find NA-type behaviour for  $b > 30$ . This is illustrated in Figs. 2 and 3, where we present the critical value  $a_{\text{cr}} - 1$  and the ratio  $x_*/x_0$  as functions of  $b$ , respectively, in the NA-type regime. These figures should be compared to Figs. 10 and 8 of [4], respectively.

A crucial point of the numerical analysis is illustrated in Fig. 4. When for a fixed value of  $b$  in the NA-type regime the critical solution is approached, the inner minimum appears at a certain minimal value of  $a$ . In Fig. 4 we present the value of the function  $N(x)$  at the outer minimum at this certain minimal value of  $a$  (where the inner minimum appears) as a function of  $b$ . Clearly, for  $40 > b > 30$ , the inner minimum of the metric function  $N(x)$  appears only, when the value of the function  $N(x)$  at the outer minimum is already very small. Indeed, with decreasing  $b$  it is decreasing from a value on the order of  $10^{-6}$  to a value on the order of  $10^{-9}$ . Obviously, with decreasing  $b$  it becomes numerically increasingly difficult, to observe NA-type behaviour at all. As illustrated in Fig. 5 for  $b = 36.125$ , once the inner minimum is present, the value of the inner minimum of  $N(x)$  decreases rapidly with increasing  $a$ , whereas the value of the outer minimum remains practically unchanged.

Even though our numerical analysis is not accurate enough to find NA-type behaviour for  $b < 30$ , we expect it to be present until  $a_{\text{tr}} = 1.5$  is reached. Linear extrapolation of the curve in Fig. 2 leads to  $b_{\text{tr}} = 25.58$ , while (a less accurate) extrapolation of the curve in Fig. 4 leads to  $b_{\text{tr}} = 26.7$  [7]. Thus our numerical analysis strongly supports the analytical result of Lue and Weinberg [4].

What concerns their numerical results, we fully agree with their explicit calculations as far as presented in [4]. However, Lue and Weinberg do not consider numerical solutions, where the value of the outer minimum is smaller than  $10^{-6}$  [4,8]. Thus they miss NA-type solutions for values of  $b$  smaller than about 40, as seen from Fig. 4. Indeed, if we extract from our numerical data a modified “critical” value of  $a$  by requiring that the value of the minimum of  $N(x)$  should be  $10^{-6}$  [8] instead of requiring that it should be zero, we obtain full agreement with Fig. 10 of Lue and Weinberg [4].

#### IV. BLACK HOLES

We now turn to the black hole solutions of the SU(2) EYMH system. Imposing again the condition of asymptotic flatness, the black hole solutions satisfy the same boundary conditions at infinity as the regular solutions. The existence of a regular event horizon at  $x_h$  requires

$$\mu(x_h) = \frac{x_h}{2}, \quad (20)$$

and  $A(x_h) < \infty$ , and the matter functions must satisfy

$$N' K'|_{x_h} = K \left( \frac{K^2 - 1}{x^2} + H^2 \right) \Big|_{x_h}, \quad (21)$$

and

$$x^2 N' H'|_{x_h} = H (2K^2 + \beta^2 x^2 (H^2 - 1)) \Big|_{x_h}. \quad (22)$$

Magnetically charged non-abelian black hole solutions exist only in a limited region of the  $(a, x_h)$  plane [1–3], as illustrated for instance for  $b = 0$  in Fig. 7 of [2]. When  $a$  is varied, while  $b$  and the horizon radius  $x_h$  are kept fixed, magnetically charged non-abelian black holes also approach critical solutions [1–3].

Extending the above analysis to the case of black holes, we observe again two regimes of  $b$ , each with its own type of critical solution corresponding to NA-type and RN-type behaviour, respectively. Since the transition value  $a_{\text{tr}} = 1.5$  is obtained by performing a Taylor expansion about a point “far” from the horizon and by making use of the first few terms of this expansion, we expect this result to hold also in the case of black holes.

Our numerical results for black holes with horizon radius  $x_h = 0.01$  and  $0.1$  are included in Figs. 2–4, along with the corresponding results for the regular solutions. We observe a complete analogy of the results for regular solutions and black holes. With increasing horizon radius  $x_h$ , the transition occurs for decreasing values of  $b$ . Extrapolating the curves of Fig. 2 to  $a_{\text{tr}} = 1.5$ , we find  $b_{\text{tr}} \approx 24$  for  $x_h = 0.01$  and  $b_{\text{tr}} \approx 15$  for  $x_h = 0.1$  [9].

Finally, in Fig. 6 we present  $x_*/x_0$  as a function of the horizon radius  $x_h$  for  $b = 12.5$ ,  $b = 21.125$ ,  $b = 32$  and  $b = 50$ . For  $b = 12.5$  and  $b = 21.125$  the monopole solutions show RN-type behaviour. This behaviour extends to the black hole solutions for  $b = 12.5$  up to  $x_h \leq 0.17$  and for  $b = 21.125$  up to  $x_h \leq 0.07$ . The precise transition value must be extrapolated [10]. For larger values of  $x_h$  NA-type behaviour arises. For  $b = 32$  and  $b = 50$  regular and black holes solutions show NA-type behaviour. (For  $b = 105$  and  $x_h = 0.1$  only the second minimum is left, as compared to  $b \geq 400$  for the regular solutions [4].) For larger values of  $b$  and horizon radius  $x_h > 0.3$  the analysis of black holes solutions needs special consideration [3].

## V. CONCLUSION

For gravitating monopoles and non-abelian black holes we have studied numerically the transition between the low and the high Higgs mass regime. Considering the approach of the solutions towards a limiting critical solution, the low Higgs mass regime shows RN-type behaviour, i.e. the critical solution where a horizon first appears corresponds to an extremal RN solution outside the horizon, while it is non-singular inside. In contrast, the high Higgs mass regime shows NA-type behaviour, i.e. the critical solution is an extremal black hole with non-abelian hair. In particular, analytical analysis suggests that RN-type behaviour should not occur for  $a < a_{\text{tr}} = 1.5$  corresponding to  $b > b_{\text{tr}} \approx 25.6$  [4].

Our numerical analysis indicates two main results:

- For asymptotically flat gravitating monopoles NA-type behaviour is still present at  $b = 30$ , considerably below the numerical value given by Lue and Weinberg [4]. We strongly expect that the NA-type behaviour persists until the analytical transition value is reached. But our numerical accuracy is insufficient to show this other than by extrapolation.
- The analogous phenomenon occurs for black hole solutions. Here with increasing values of the horizon radius  $x_h$ , the transition occurs for decreasing values of  $b$ .

## VI. APPENDIX

We employ a collocation method for boundary-value ordinary differential equations developed by Ascher, Christiansen and Russell [11]. The set of non-linear coupled differential equations eqs. (10) - (13) is solved using the damped Newton method of quasi-linearization. At each iteration step a linearized problem is solved by using a spline collocation at Gaussian points. Since the Newton method works very well, when the initial approximate solution is close to the true solution, the gravitating monopole solutions for varying parameters  $a$  and  $b$  are obtained by continuation.

The linearized problem is solved on a sequence of meshes until the required accuracy is reached. For a particular mesh  $x_i = x_1 < x_2 < \dots < x_{N+1} = x_o$ , where  $x_i$  and  $x_o$  are the boundaries of the interval, and  $h_i = x_{i+1} - x_i$ ,  $h = \max_{1 \leq i \leq N} h_i$ , a collocation solution  $\vec{v}(x) = (v_1, v_2, \dots, v_d)$  is determined. Each component  $v_n(x) \in C^{m_n-1}[x_i, x_o]$ , is a polynomial of degree smaller than  $k + m_n$ , where  $m_n$  is the order of the  $n$ -th equation, and  $k$  is an integer bigger than the highest order of any of the differential equations. The collocation solution is required to satisfy the set of differential equations at the  $k$  Gauss-Legendre points in each subinterval as well as the set of boundary conditions.

When approximating the true solution  $u_n(x)$  by the collocation solution  $v_n(x)$ , an error estimate in each subinterval  $x \in [x_i, x_{i+1}]$  is obtained from the expression

$$\|u_n^{(l)}(x) - v_n^{(l)}(x)\|_{(i)} = c_{n,l} |u_n^{(k+m_n)}(x_i)| h_i^{k+m_n-l} + O(h^{k+m_n-l+1}) \quad (23)$$

$$l = 0, \dots, m_n - 1, \quad n = 1, \dots, d, \quad (24)$$

where  $c_{n,l}$  are known constants. Also, using eq. (24) a redistribution of the mesh points is performed to roughly equidistribute the error. With this adaptive mesh selection procedure, the equations are solved on a sequence of

meshes until the successful stopping criterion is reached, where the deviation of the collocation solution from the true solution is below a prescribed error tolerance [11].

For the gravitating monopole solutions, we typically specified the error tolerance in the range  $10^{-4} - 10^{-6}$ , but the absolute errors of the collocation solutions normally turned out to be far better, e.g. in the range  $10^{-7} - 10^{-12}$ . The number of mesh points used in these calculations was typically about 350, with nearly 70% of the mesh points in the critical region of the two minima of  $N(x)$ , if present.

We calculated the solutions on the finite interval  $[0, x_o]$  with  $x_o$  ranging from 10 to  $10^4$ . The solutions are highly independent of the size of the interval, as seen in Fig. 7, where the metric function  $N(x)$  is shown for the parameters  $a = 1.43596$ ,  $b = 36.125$  and three value of  $x_o$ . Indeed, as specified by their boundary conditions eqs. (17)-(18), the gravitating monopole solutions are asymptotically flat.

In Fig. 5, where the evolution of the two minima of the metric function  $N(x)$  is shown for  $b = 36.125$ , the corresponding global error estimates for the function  $N(x)$  are also shown.

For the black hole solutions the set of boundary conditions eqs. (20)-(22) is employed, and the calculations are performed on an interval  $[x_h, x_o]$ , where  $x_h$  represents the horizon of the black hole. The error tolerances and the errors are comparable to those of the gravitating monopole solutions.

- [1] K. Lee, V.P. Nair and E.J. Weinberg, Black holes in magnetic monopoles, *Phys. Rev. D* 45 (1992) 2751.
- [2] P. Breitenlohner, P. Forgacs and D. Maison, Gravitating monopole solutions, *Nucl. Phys. B* 383 (1992) 357.
- [3] P. Breitenlohner, P. Forgacs and D. Maison, Gravitating monopole solutions II, *Nucl. Phys. B* 442 (1995) 126.
- [4] A. Lue and E.J. Weinberg, Magnetic monopoles near the black hole threshold, *Phys. Rev. D* 60 (1999) 084025.
- [5] Y. Brihaye, B. Hartmann, J. Kunz, Gravitating dyons and dyonic black holes, *Phys. Lett. B* 441 (1998) 77.
- [6] Y. Brihaye, B. Hartmann, J. Kunz, and N. Tell, Dyonic non-abelian black holes, *Phys. Rev. D* 60 (1999) 104016.
- [7] We obtained a decent fit for the lower  $b$  points with  $\log N_{\min} = -1.5/(x - 26.7)^{0.37}$ .
- [8] A. Lue and E.J. Weinberg, private communication.
- [9] Extrapolation of the curves of Fig. 3 (see [7]) leads to  $b_{\text{tr}} \approx 25$  for  $x_h = 0.01$  and  $b_{\text{tr}} \approx 16$  for  $x_h = 0.1$ .
- [10] Extrapolation of the upper two curves of Fig. 6 leads to the transition values  $x_h \approx 0.14$  and  $x_h \approx 0.03$  for  $b = 12.5$  and  $b = 21.125$ , respectively.
- [11] U. Ascher, J. Christiansen, R. D. Russell, A collocation solver for mixed order systems of boundary value problems, *Mathematics of Computation* 33 (1979) 659;  
U. Ascher, J. Christiansen, R. D. Russell, Collocation software for boundary-value ODEs, *ACM Transactions* 7 (1981) 209.

## Figure captions

Fig. 1

The metric function  $N(x)$  is presented in the NA-type regime for  $b = 36.125$  and  $a = 1.43482, 1.43550, 1.43583$  and  $1.43596$ .

Fig. 2

The critical value  $a_{\text{cr}} - 1$  is presented as a function of  $b$  in the NA-type regime for monopole solutions and for black hole solutions with horizon radii  $x_h = 0.01$  and  $0.1$ .

Fig. 3

The ratio  $x_*/x_0$  is presented as a function of  $b$  in the NA-type regime for monopole solutions and for black hole solutions with horizon radii  $x_h = 0.01$  and  $0.1$ .

Fig. 4

The value of the metric function  $N(x)$  at the outer minimum at the minimal value of  $a$  where the inner minimum appears is presented as a function of  $b$ , for monopole solutions and for black hole solutions with horizon radii  $x_h = 0.01$  and  $0.1$ .

Fig. 5

The values of the metric function  $N(x)$  at the outer minimum and at the inner minimum are presented as a function of  $a$  close to  $a_{\text{cr}}$  for  $b = 36.125$ . Also shown is the global error estimate for  $N(x)$ .

Fig. 6

The ratio  $x_*/x_0$  is presented for black hole solutions as a function of  $x_h$  in the NA-type regime for the values  $b = 12.5, 21.125, 32$ , and  $50$ , corresponding to  $\beta = 5, 6.5, 8, 10$ .

Fig. 7

The metric function  $N(x)$  is presented in the NA-type regime for  $b = 36.125$  and  $a = 1.43596$ , as obtained on the interval  $[0, x_0]$  with  $x_0 = 10, 1000, 10000$ . (The three curves cannot be distinguished graphically.)

**Figure 1**

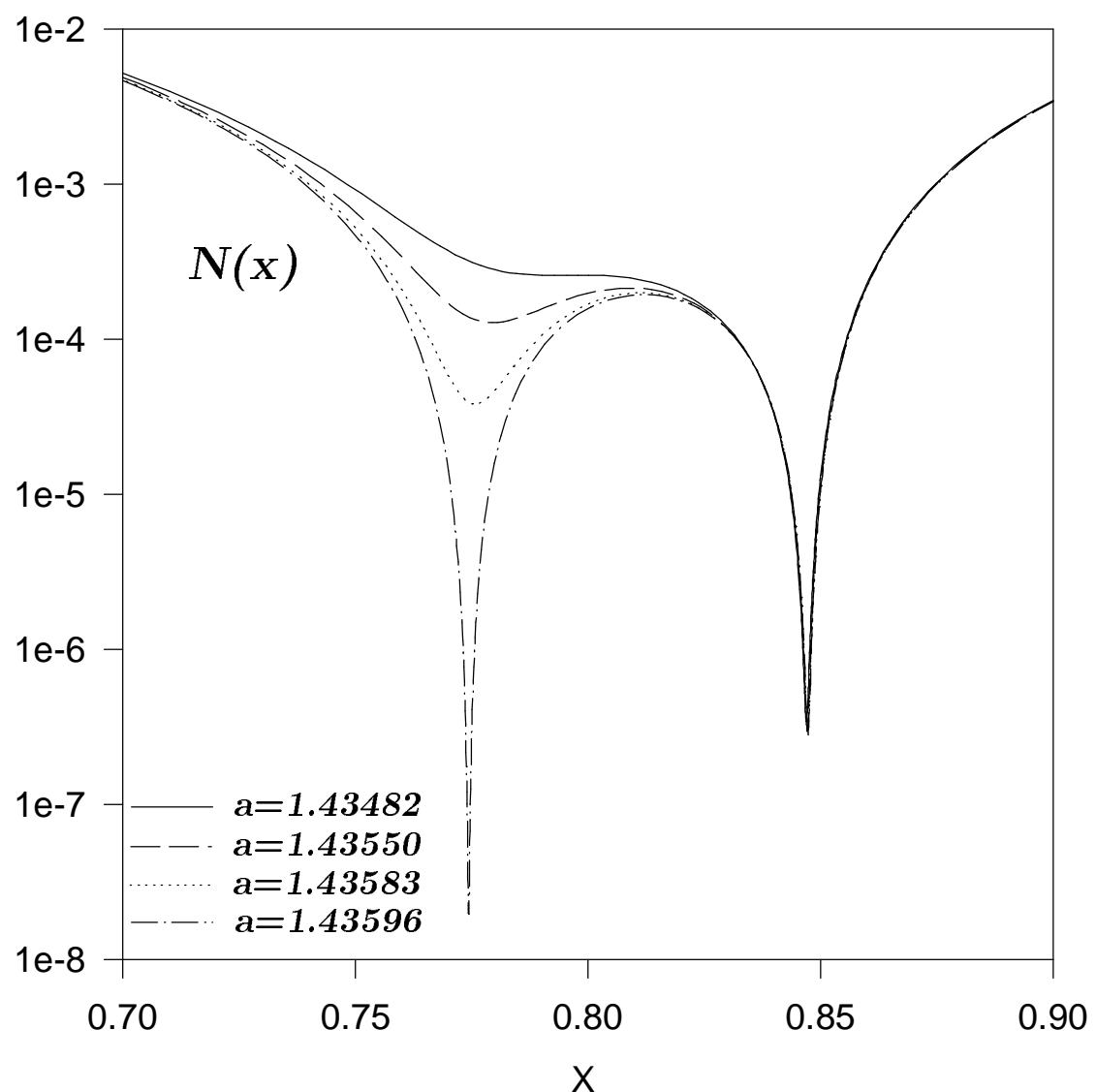


**Figure 2**

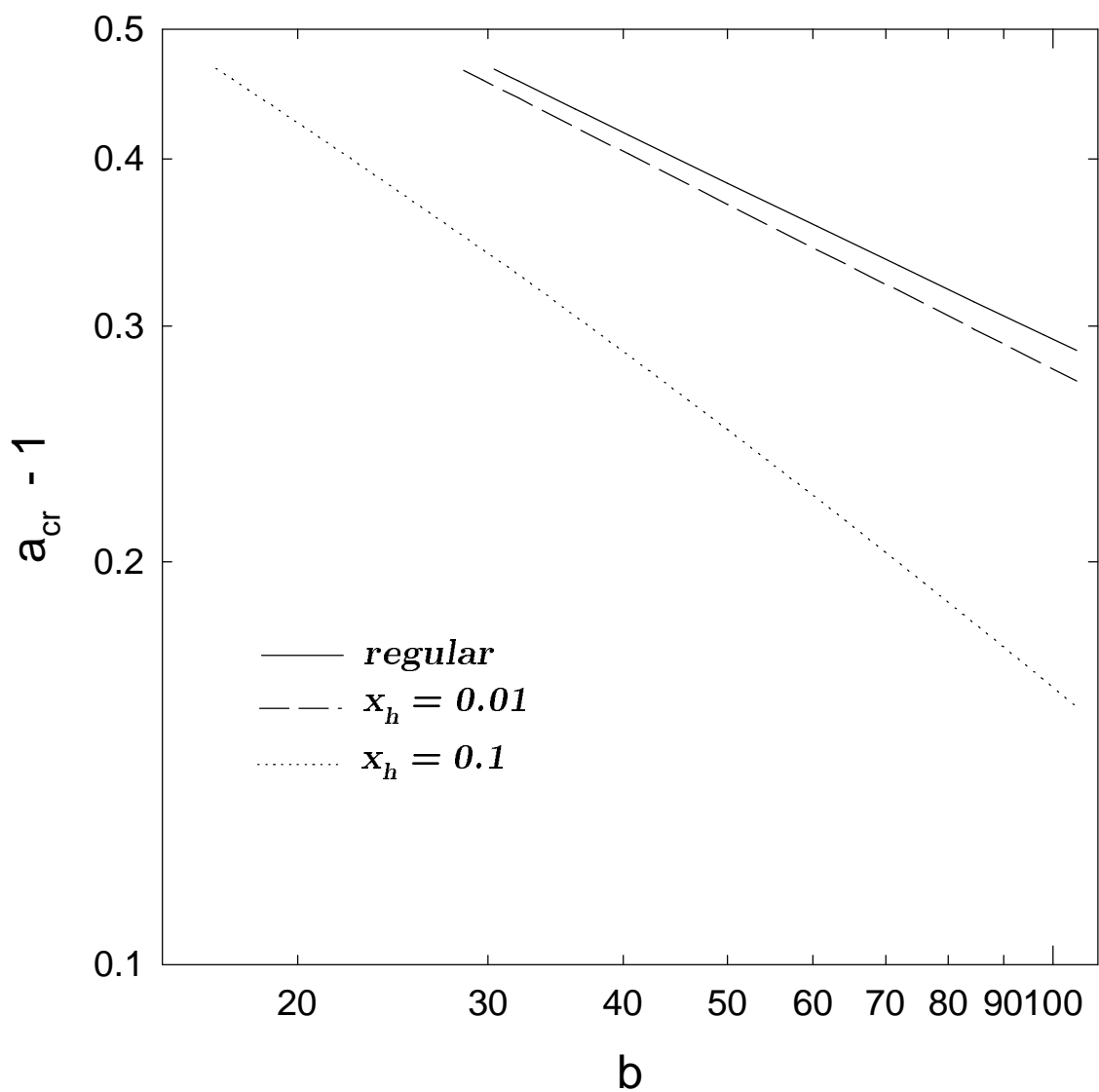


*Figure 3*

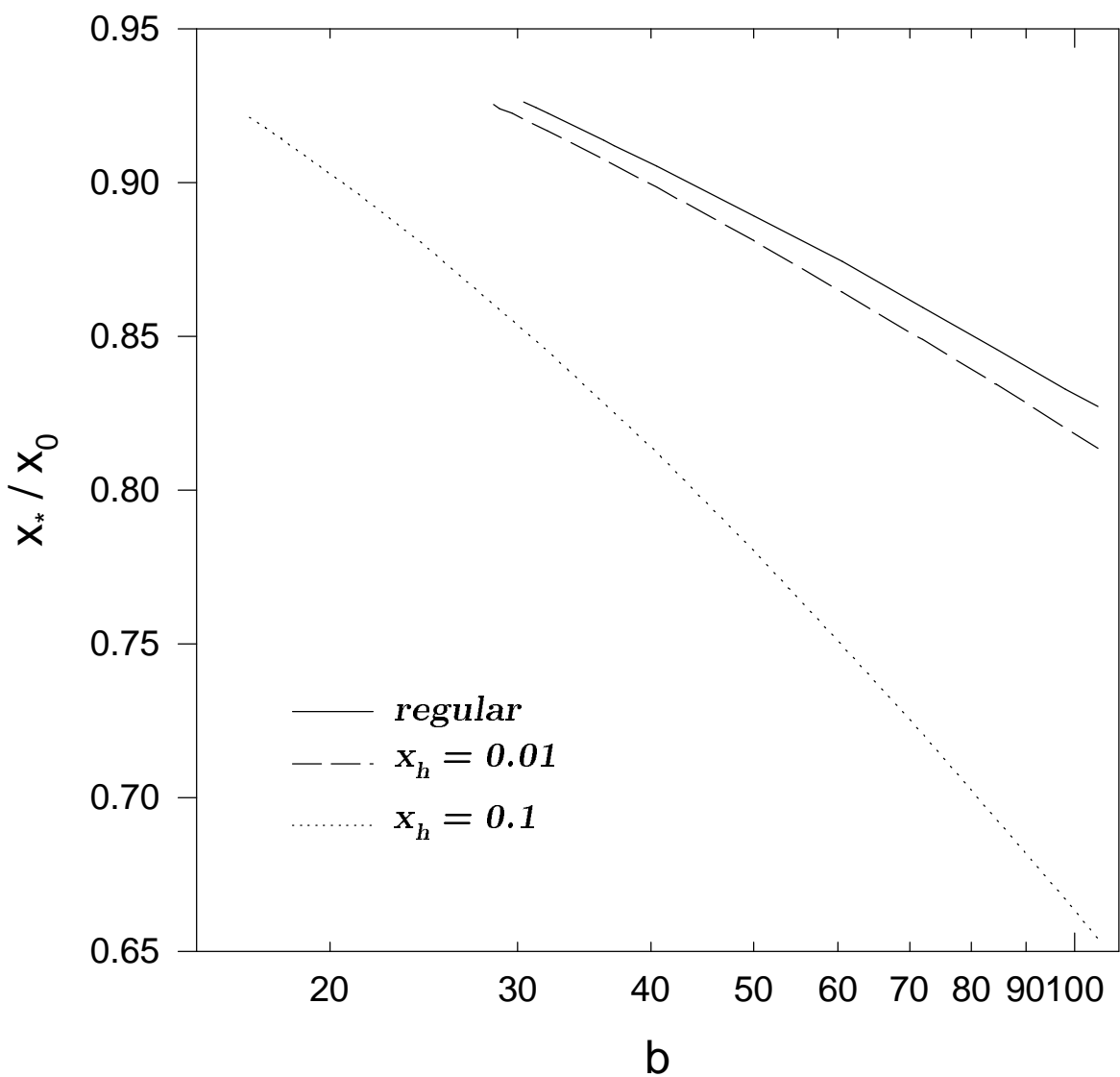


**Figure 4**

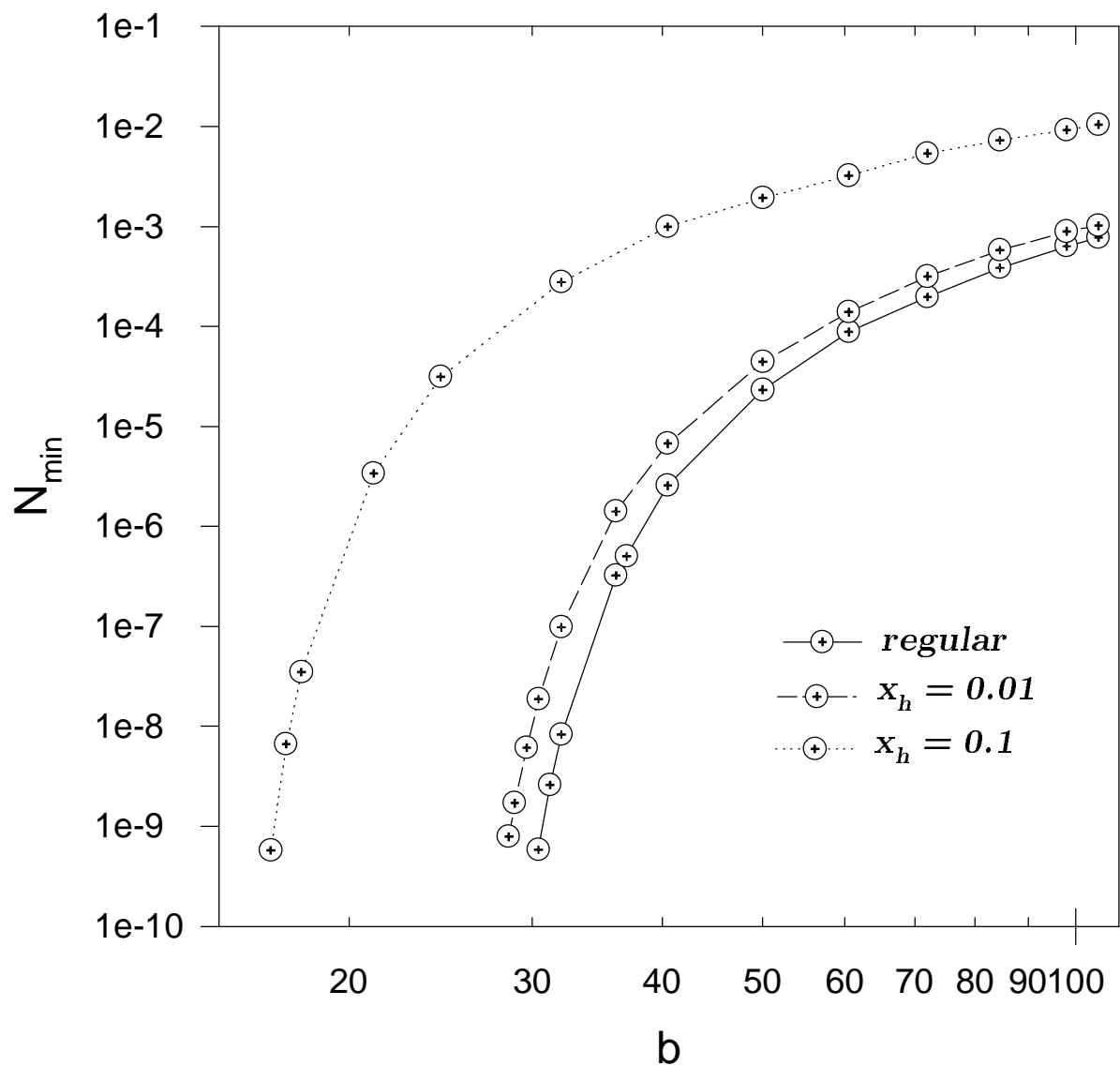


*Figure 5*

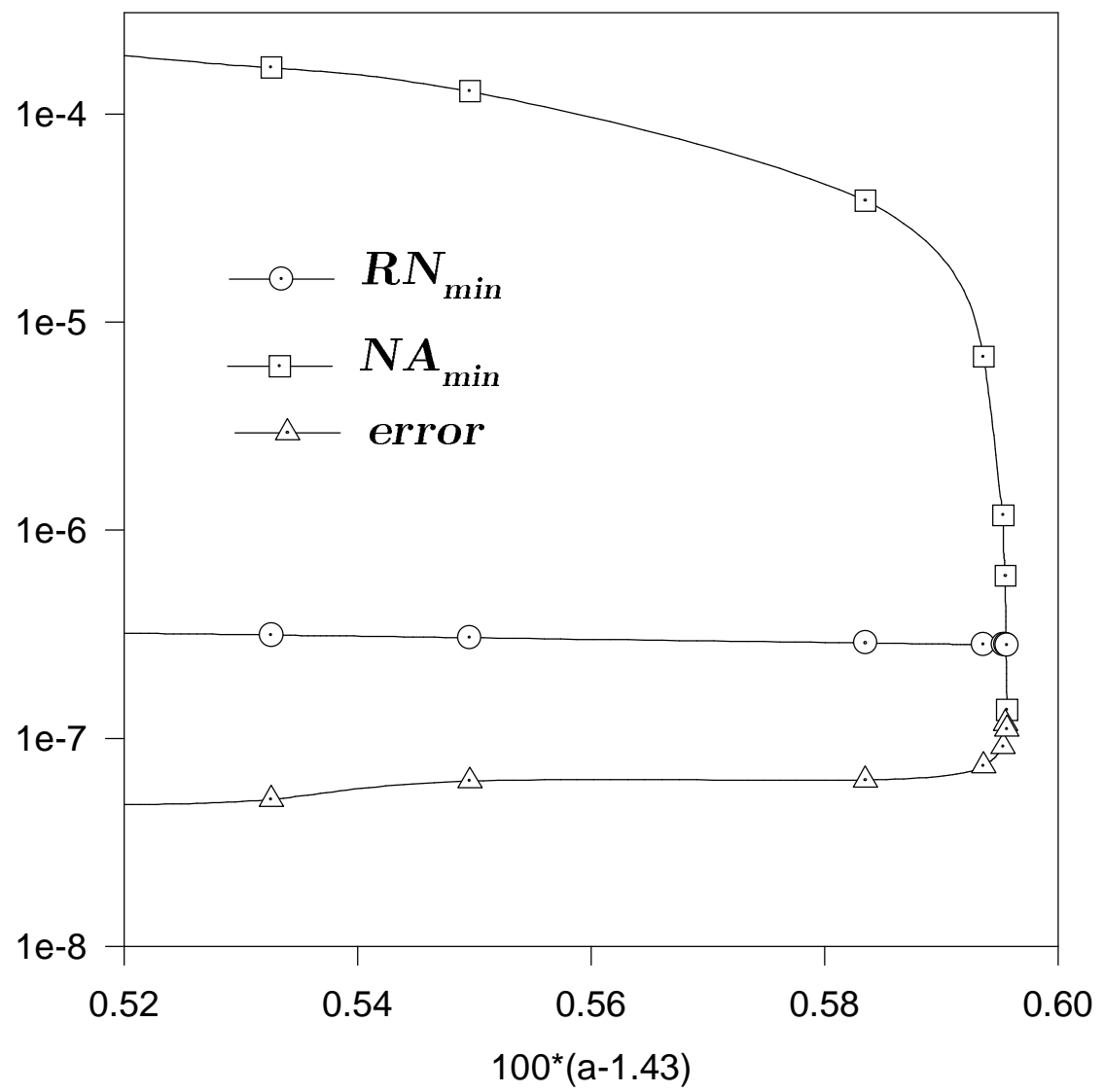


**Figure 6**

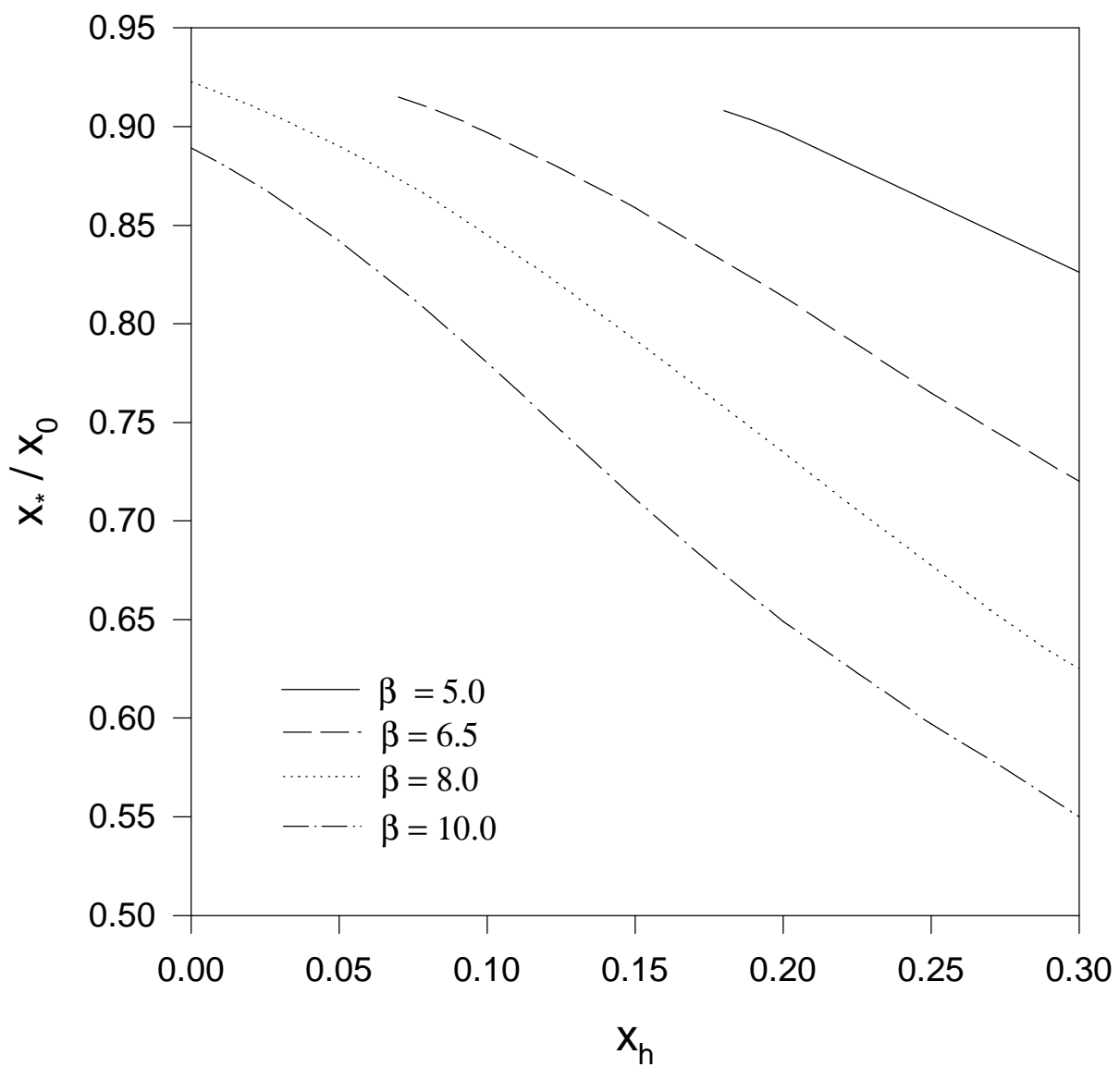


*Figure 7*

